PNAS RESEARCH ARTICLE | ECOLOGY

Permafrost instability negates the positive impact of warming temperatures on boreal radial growth

Raquel Alfaro-Sánchez[a,b,1], Andrew D. Richardson[c,d], Sharon L. Smith[e], Jill F. Johnstone[f,g], Merritt R. Turetsky[h], Steven G. Cumming[i], James M. Le Moine[j], and Jennifer L. Baltzer[b]

Affiliations are included on p. 10.

Edited by Eric Rignot, University of California Irvine, Irvine, CA; received June 12, 2024; accepted October 1, 2024

Climate warming can alleviate temperature and nutrient constraints on tree growth in boreal regions, potentially enhancing boreal productivity. However, in permafrost environments, warming also disrupts the physical foundation on which trees grow, leading to leaning trees or "drunken" forests. Tree leaning might reduce radial growth, undermining potential benefits of warming. Here, we found widespread radial growth reductions in southern latitude boreal forests since the 1980s. At mid latitudes, radial growth increased from ~1980 to ~2000 but showed recent signs of decline afterward. Increased growth was evident since the 1980 s at higher latitudes, where radial growth appears to be temperature limited. However, recent changes in permafrost stability, and the associated increased frequency of tree leaning events, emerged as a significant stressor, leading to reduced radial growth in boreal trees at the highest latitudes, where permafrost is extensive. We showed that trees growing in unstable permafrost sites allocated more nonstructural carbohydrate reserves to offset leaning which compromised radial growth and potential carbon uptake benefits of warming. This higher allocation of resources in drunken trees is needed to build the high-density reaction wood, rich in lignin, that is required to maintain a vertical position. With continued climate warming, we anticipate widespread reductions in radial growth in boreal forests, leading to lower carbon sequestration. These findings enhance our understanding of how climate warming and indirect effects, such as ground instability caused by warming permafrost, will affect boreal forest productivity in the future.

climate warming | tree leaning | reaction wood | stemwood non-structural carbohydrates | permafrost

Significance

In boreal forests, short growing seasons, cold temperatures, and the presence of frozen ground (permafrost) limit tree growth. Climate warming can potentially enhance growth by increasing air and soil temperatures. Here, we found reduced tree growth since the 1980 s at southern latitudes and increased growth at higher, colder latitudes, at least until the 2000 s. Our results showed that recent permafrost warming at the highest latitudes, where permafrost is more prevalent in the landscape, has caused significant stress in tree growth due to ground destabilization. Trees growing in unstable permafrost used their nutrient uptake to remain upright instead of increasing their growth. These findings indicate that boreal forests will not become more productive with climate warming and the resulting permafrost thaw.

The boreal biome houses 30 to 40% of terrestrial carbon stocks (1) and provides critical ecosystem services, such as wood production and carbon storage, that have impacts at local, regional, and global scales (2). About 80% of the boreal biome lies within the permafrost region (3), with the majority in the zone of discontinuous permafrost, where permafrost is patchy in the landscape. Boreal ecosystems are warming at three to four times the global mean rate due to Arctic amplification (4, 5). Permafrost temperatures are also increasing (6), particularly in colder permafrost at higher latitudes (7), and it is virtually certain that permafrost thaw will increase and permafrost extent will decrease under continued global warming (8). However, it is unknown how these combined effects of climate change will impact growth trajectories in boreal trees and whether these changes in growth might offset or compound predicted carbon losses from warming soils.

In the context of warming temperatures, there is a fundamental debate around the degree to which carbon assimilation via photosynthesis (i.e., carbon source limitation) versus direct environmental limitations to cambial cell development (i.e., growth or carbon sink limitation) controls radial growth (9). In cold-adapted plants, the capacity for wood tissue formation becomes marginal at temperatures below 5 °C (10–12), pointing toward the carbon sink limitation hypothesis as the main driver of growth, i.e., that low temperatures constrain tree growth despite sufficient photosynthesis. Additionally, widespread permafrost thaw may benefit the functioning of overlying forests, mainly due to warmer soils and deeper permafrost tables (13, 14) that support greater soil resource availability and rooting volume (15–17). Moreover, the release of previously inaccessible resources from thawing permafrost may enhance tree productivity (16, 18), at least in the short term (19)—although more research is needed as previous studies have focused mostly on experimentally induced permafrost thaw rather than direct field observations, and not on mature trees (20, 21). Consequently, trees at higher latitudes are expected to increase their radial growth primarily as a response to higher air and soil temperatures, extended growing season lengths, and greater thaw depths.

Author contributions: R.A.-S., S.L.S., J.F.J., M.R.T., S.G.C., and J.L.B. designed research; R.A.-S., A.D.R., and J.M.L.M. performed research; R.A.-S., S.L.S., S.G.C., and J.L.B. analyzed data; and R.A.-S., S.L.S., J.F.J., S.G.C., and J.L.B. wrote the paper.

The authors declare no competing interest.

This article is a PNAS Direct Submission.

[1]To whom correspondence may be addressed. Email: raquel.alfarosanchez@nrcan-rncan.gc.ca.

This article contains supporting information online at https://www.pnas.org/lookup/suppl/doi:10.1073/pnas.2411721121/-/DCSupplemental.

Published December 2, 2024.

Analysis of satellite imagery reveals greening primarily in the coldest margins of the boreal biome (22). Ultimately, an overall greening may enhance carbon uptake, relieving or even offsetting the loss of carbon that will occur as permafrost thaws, as seen in the Tibetan Plateau (23). However, warmer margins of the boreal biome are exhibiting reductions in carbon sequestration and plant growth and increases in mortality, known as "boreal browning" (22, 24–26). Browning could result from an increase in evapotranspirative demand or reduced soil moisture, leading to drought stress in trees. Projected increases in water loss via evapotranspiration could force the trees to reduce their photosynthetic carbon uptake by partial stomatal closure. Decreased photosynthesis leads to carbon depletion in sink tissue and a reduction in tree growth as a mechanism to reduce the risk of carbon starvation and hydraulic failure (27). Browning could also result from drought responses owing to changes in rooting-zone soil moisture conditions following thaw (15, 28–30).

Another extensive, yet often overlooked, disturbance affecting tree growth that is common in permafrost environments is ground instability caused by seasonal and long-term changes in ice-rich permafrost, which causes trees to lean off-vertical (31–34). In permafrost environments of boreal North America, the widespread conifer black spruce [*Picea mariana* (Mill.) B.S.P.] dominates forested peatlands (35), where it occupies extensive regions of leaning trees known as "drunken" forests. Radial growth in leaning trees is altered due to the formation of reaction wood, which counteracts the tree tilting associated with the physical destabilization of permafrost. Therefore, periods of increased frequency of tilting in boreal conifers growing in areas with frost-susceptible sediments can often be attributed to changes in active layer (seasonally thawed) thickness (ALT) (32, 33).

A better understanding of how the complex abiotic interactions that northern boreal trees experience may alter radial growth and carbon reserves requires combining physiological approaches with tree ring and environmental data (36–39). Nonstructural carbohydrates (NSCs) provide insights into the conditions under which growth is constrained by the environment versus actively reduced by the plant and how the mobilization of carbon stores affects productivity of the trees (40). Thus, the study of NSC (mainly sugars and starch) distribution across stemwood tree rings can help elucidate whether reserves deep in the stem are metabolically active and available to support functional processes and how stemwood NSC distribution varies with abiotic factors, such as increased temperatures, drought stress, or the physical destabilization observed on permafrost environments. The cold conditions of near-surface permafrost sites are a well-documented example of stress in trees that lead to elevated concentrations of NSCs (41) at the expense of radial growth, but this conservative approach may be susceptible to change with warming. Impacts of other stressful environmental conditions such as the increased destabilization of permafrost tables on tree productivity and resource allocation remain unexplored.

Here, we evaluated the effects of permafrost and climate variability and the occurrence of tree leaning events on black spruce radial growth (tree-ring widths, TRW) across a 650 km climatic and permafrost gradient in the Northwest Territories, Canada. We used permafrost monitoring sites that provided historic records of seasonal thaw to investigate the link between the occurrence of tree leaning events and permafrost table stability (ground stability). To gain insight into the availability of carbon reserves in black spruce trees, we examined radial patterns of stemwood NSCs, and their relationship with TRW, in trees growing over contrasting permafrost table depth and stability conditions.

Results

Effects of Near-Surface Permafrost Presence and Climate Variability on Radial Growth Trajectories. To determine how the presence or absence of near-surface permafrost and climate variability affected TRW, we analyzed black spruce radial growth patterns in 109 sites from 1940 to 2020. Study sites spanned the low subarctic Taiga Plains in the North (N), the mid and high boreal Taiga Plains in the South (S), and the Taiga Shield (hereafter N Plains, S Plains, and Shield; Fig. 1*A* and *SI Appendix*, Fig. S1 and Table S1*A*). Over the period from 1940–2020, no significant differences in TRW were observed in the Plains when comparing sites with near-surface permafrost (permafrost table shallower than 2 m, i.e., within the rooting zone—and potentially impacting trees growing over them) and sites with no permafrost or deep permafrost (permafrost table deeper than 2 m, i.e., below the rooting zone). On the Shield, TRW was significantly higher in sites with no or deep permafrost than in sites with near-surface permafrost since ~1980 s (Fig. 1*B* and *SI Appendix*, Tables S4 and S5).

TRW exhibited a pattern of widespread reductions at southern latitudes and increased growth at northern latitudes. Specifically, in the southernmost ecoregion, the S Plains, TRW decreased from ~1950 to 2020. At mid latitudes, in the Shield ecoregion, TRW increased since ~1980 but showed signs of decline in the last two decades. In the northernmost ecoregion, the N Plains, TRW increased from ~1980 to 2020 (*Methods*; Fig. 1*B* and *SI Appendix*, Tables S4).

TRW was most strongly associated with summer minimum air temperature (Tmin) at higher latitudes (i.e., N Plains) and with summer drought, as measured by CMD, in mid and southern latitudes (i.e., Shield and S Plains ecoregions) (*Methods*; Fig. 1*C*). Higher temperatures and lower moisture deficit enhanced TRW, particularly in sites with no or deep permafrost in the Shield. We observed a nonlinear response of TRW to Tmin in the N Plains and a nonlinear response of TRW to CMD in all three ecoregions, suggesting a deceleration in growth with continued increase in temperature or moisture deficit, respectively (*Methods*; *SI Appendix*, Fig. S2 and Table S4).

Effect of Permafrost Table Stability on Radial Growth Trajectories. We investigated how permafrost table stability affected radial growth in 15 long-term permafrost monitoring sites in the N Plains. These sites provided annual records of ALT (*Methods*) from 2008 to 2018–2019. The permafrost monitoring sites showed consistent increases in ALT (i.e., permafrost thaw) over the period studied (median thaw rate in the near-surface permafrost sites 5.3 cm y^{-1}), although some plots also showed permafrost aggradation (*SI Appendix*, Fig. S3). We converted the site-level ALT rates into absolute rates of permafrost change to obtain a measurement of permafrost table stability, where higher absolute rates indicated greater ground instability, owing either permafrost thaw or aggradation processes (*Methods*). We found significant reductions in TRW with greater absolute rates of permafrost change over the period of 2008–2020 (Fig. 2*A* and *SI Appendix*, Table S6*A*).

Considering that higher absolute thaw or aggradation rates may have greater impact on trees when occurring within the rooting zone, we classified the permafrost monitoring sites into four permafrost categories, based on their permafrost table depth and stability (*Methods*): i) deep stable, ii) near-surface stable, iii) deep unstable, or *iv*) near-surface unstable permafrost sites. Over the period of 2008–2020, greater TRW was observed in the

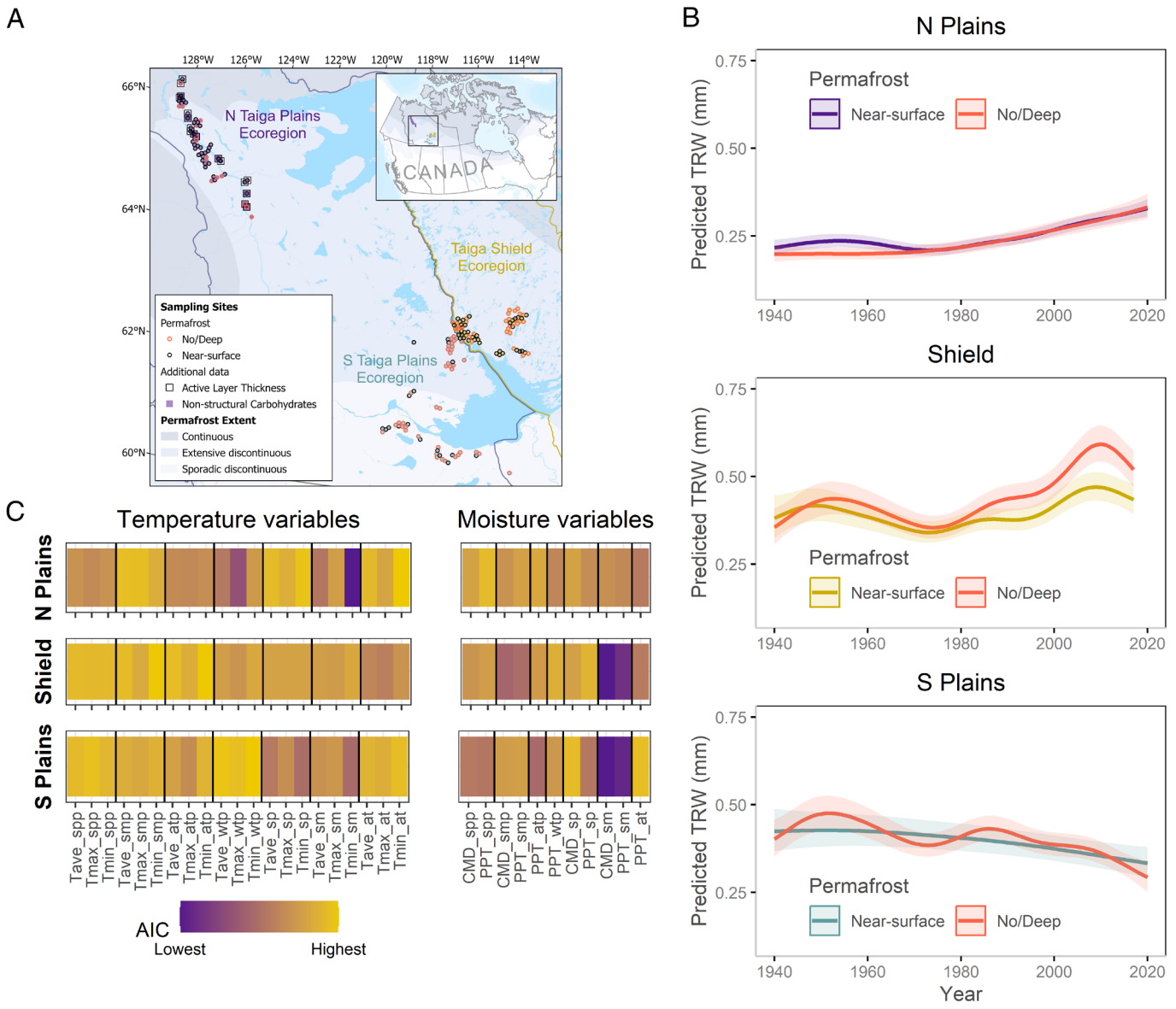

Fig. 1. Location map, radial growth trajectories, and climate-growth sensitivity. (*A*) Map of sampling sites within three ecoregions, the low subarctic Northern Taiga Plains ecoregion (N Plains), the high-mid boreal Southern Taiga Plains ecoregion (S Plains), and the Taiga Shield ecoregion (Shield). Different symbols indicate whether sites had near-surface permafrost (permafrost table shallower than 2 m, i.e., within the rooting zone), as well as annual records of ALT and NSC data. Points have been jittered for better visualization. Permafrost extent information obtained from ref. 42. Mapping was created using ArcGIS Pro 3.2 (*B*) Predicted TRW and 95% CI as a function of calendar year for the two-level permafrost factor, i.e., sites with near-surface permafrost or with no or permafrost deeper than two meters for each ecoregion (*SI Appendix*, Table S4). Other terms in the model are held constant at their medians. (*C*) Comparison of combined AIC values per ecoregion obtained in linear models (LMs) between individual TRW residuals with seasonal (sp, spring; sm, summer; at, autumn; and wt, winter) temperature (Tave, average air temperature; Tmin, minimum air temperature, and Tmax, maximum air temperature) and moisture (PPT, precipitation; CMD, climate moisture deficit) variables. For each seasonal variable, we used current year and previous year values (indicated with a p after the season abbreviation) from spring of the previous year to fall of the current year, and all seasonal combinations within that time frame (*SI Appendix*, Table S2). The lowest AIC values correspond to the most influential variable and seasonal window for TRW for each ecoregion (*Methods*).

permafrost monitoring sites with deep stable or near-surface stable permafrost (Fig. 2*B* and *SI Appendix*, Table S6*B*). In addition, higher air temperatures were associated with greater TRW only in the permafrost monitoring sites with deep stable permafrost, suggesting a deceleration in growth in sites with unstable or near-surface permafrost (*SI Appendix*, Fig. S4 and Table S6*B*). No significant differences in TRW were found with respect to permafrost depth conditions (i.e., near-surface stable or unstable vs deep stable or unstable permafrost) in the permafrost monitoring sites (*SI Appendix*, Tables S6*B* and S7). This result is consistent with our findings for the N Plains over the period from 1940 to 2020, where no significant differences were observed based on permafrost conditions at the time of sampling (*SI Appendix*, Table S4*A*).

Frequency of Leaning Events as a Surrogate Variable for Historical Changes in Permafrost. We investigated whether the number of leaning events per tree could serve as a proxy for historical changes in permafrost in sites lacking instrumental data on seasonal thaw rates over time. The total number of leaning events per tree was estimated based on their annual lean intensity for all trees across the latitudinal gradient with basal disk samples (*Methods*; *SI Appendix*, Table S1*A*). We found that older trees experienced a higher number of leaning events (Spearman correlations $r_s = 0.62$, $t = 19.1$, df = 568, $P < 0.001$). On average, 81% of the trees exhibited at least one leaning event, and the presence or absence of leaning events in the trees was not driven by permafrost depth conditions (*SI Appendix*, Table S8*A*). The total

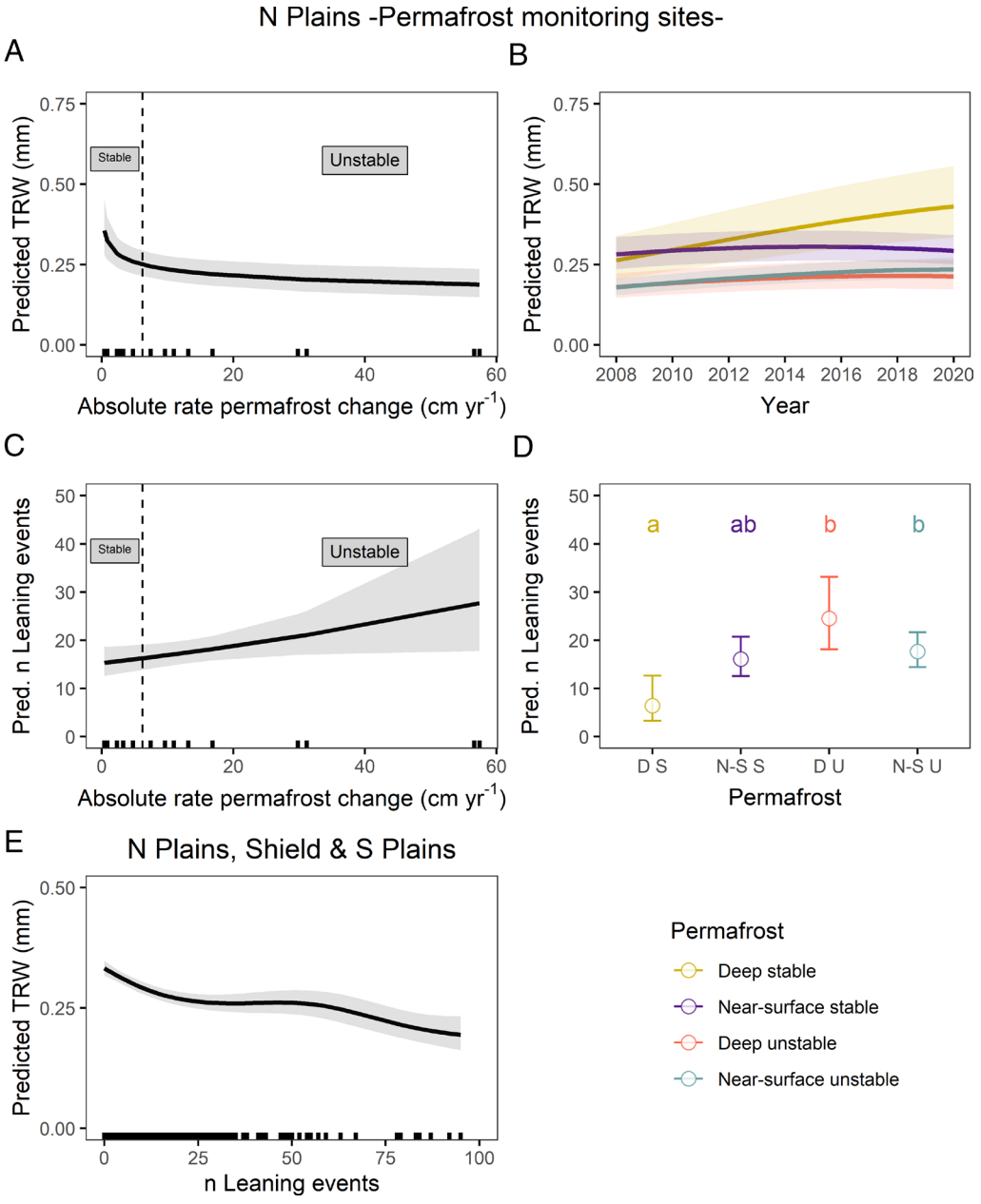

Fig. 2. Permafrost changes effects on radial growth and frequency of leaning events. Predicted TRW and 95% CI as a function of (*A*) absolute rate of permafrost change (*SI Appendix*, Table S6*A*) and as a function of (*B*) calendar year for the four levels of permafrost factor, i.e., sites with deep stable, near-surface stable, deep unstable, or near-surface unstable permafrost (*SI Appendix*, Table S6*B*). Predicted number of leaning events and 95% CI as a function of (*C*) absolute rate of permafrost change (*SI Appendix*, Table S8*B*) and as a function of (*D*) the four levels of permafrost factor (*SI Appendix*, Table S8*C*). Predicted TRW and 95% CI as function of (*E*) number of leaning events (*SI Appendix*, Table S9). For all predicted variables, other terms in the models are held constant at their medians. Black inset ticks in the x-axis on panels *A*, *C*, and *E* indicate the frequency of data. Vertical dashed lines in panels *A* and *C* indicate the threshold between stable and unstable permafrost tables (*Methods*). Lowercase letters in panel *D* indicate significant differences obtained in post hoc analyses.

number of leaning events per tree in the Shield was significantly greater in sites with near-surface permafrost conditions, but no significant differences were observed in the Plains (*SI Appendix*, Fig. S5 and Table S8*A*). However, we found that the number of leaning events in the N Plains permafrost monitoring sites significantly increased with rates of permafrost change, i.e., in sites with unstable permafrost conditions (Fig. 2 *C* and *D* and *SI Appendix*, Table S8 *B* and *C*), indicating the potential of this variable as a proxy for determining historical site permafrost table stability. We subsequently examined the impact of leaning events on TRW across the entire latitudinal gradient, where 94 out of 109 sites had no historical information about changes in permafrost. We found that TRW was significantly reduced with increased frequency of leaning events (*Methods*; Fig. 2*E* and *SI Appendix*, Tables S9). Sensitivity analyses examining the interaction between climate stress and the occurrence of leaning events on TRW revealed a cumulative negative effect on growth with increased tree leaning and climate stress in the Plains—warming in the N Plains or moisture deficit in the S Plains. However, no significant interaction effect was found in the Shield ecoregion (*SI Appendix*, Fig. S6 and Table S10).

NSCs to Unravel the Mechanism Underlying Radial Growth Response to Changes in Permafrost. To gain insight into the availability of carbon reserves in black spruce trees growing in sites experiencing changes in permafrost conditions and their relationship with TRW, we examined radial NSC (sugars) concentrations in the outermost 13 individual rings (from 2008

to 2020) in a subset of trees from the 15 long-term permafrost monitoring sites (*Methods*).

Sugar content was highest in the outermost ring, i.e., the 1-y-old ring (1.87 ± 0.36%), and declined radially toward the inner rings (0.3 ± 0.16% in the 13-y-old ring). The reduction in sugar concentration in the 13-y-old ring (the oldest ring analyzed) relative to the 1-y-old ring content was on average 83 ± 9% (*SI Appendix*, Fig. S7*A*).

We ran Pearson correlations between 1-y-old ring TRW (the outermost, last full tree ring measured) and radial content of sugars (1 to 13 y old) to investigate whether reserves deep in the stem are metabolically active and available to support functional processes such as radial growth. We found significant negative correlations between 1-y-old ring TRW and 3- to 11-y-old sugar content after Bonferroni corrections (*Methods*; Fig. 3 and *SI Appendix*, Table S11). Maximum negative correlations were found between 1-y-old ring TRW and 5- to 8-y-old sugar content (r ~ −0.81), pointing toward a higher demand for sugars to build growth from those rings. This suggests that deeper, and presumably older, sugar reserves were used to support recent growth.

Sugar content in the 1-y-old ring showed a significant positive relationship with absolute site-level rates of permafrost change (*SI Appendix*, Table S12), in contrast to the negative relationship between 1-y-old ring TRW and absolute rates of permafrost change (Fig. 2*A* and *SI Appendix*, Table S6A). This result suggests that in unstable permafrost sites (sites with higher absolute rate of permafrost change; Fig. 2*C*), more new sugars were stored and therefore not available for 1-y-old ring TRW, while in stable permafrost sites, new sugars were more available to trees for growth.

We then calculated the percentage of sugar depletion in stemwood rings from 2- to 13-y-old relative to sugar content in the 1-y-old ring and compared the percentages of sugar depletion per tree across the four levels of permafrost conditions (*Methods*). We found a significant steeper depletion in sites with deep stable permafrost, than in near-surface stable or unstable permafrost sites (Fig. 4 and *SI Appendix*, Table S13). Specifically, sugar

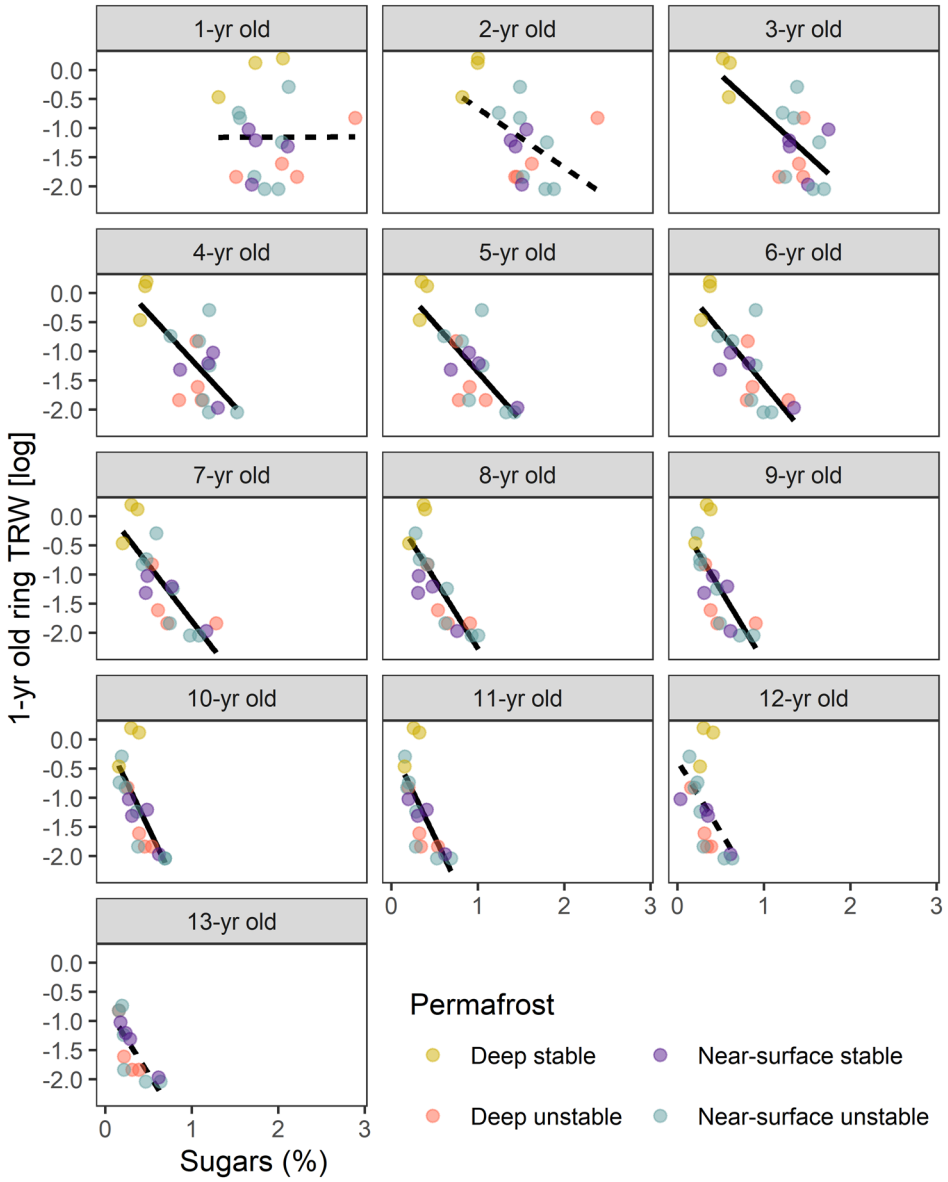

Fig. 3. Relationships between radial growth and stemwood sugar concentrations. Relationship between 1-y-old ring TRW [log-transformed] and 1 to 13-y-old ring sugar concentrations. Dashed lines indicate nonsignificant Pearson correlations for a Bonferroni critical value of $P < 0.00385$ (*Methods*; *SI Appendix*, Table S11). Points are raw tree sugar concentrations color-coded to indicate the four levels of permafrost factor.

concentrations decreased from the 1-y-old to the 2-y-old ring by 43.7 ± 7% in sites with deep stable permafrost, compared to a decrease of 19.5 ± 11.9% in deep unstable sites, 17.3 ± 11.6% in near-surface stable sites or 12.4 ± 10.2% in near-surface unstable sites. Differences in the percentage of sugar depletion among the four permafrost condition levels were more notable between the 2nd- and the 5th-y-old rings (Fig. 4 and *SI Appendix*, Table S13).

Discussion

While rising levels of atmospheric CO_2 make more carbon available for photosynthesis, additional factors or conditions are required to allow trees to take advantage of this extra carbon through enhanced tree growth (43). In cold-adapted conifers, the allocation of assimilated carbon to structural investment, i.e., tissue growth, is hindered when air temperatures fall below 5 °C (12). Since the 1980 s, warming has relaxed temperature constraints on radial growth at high latitudes (39, 44). This response is evident in our sites within the N Plains and the Shield (until the last two decades), two ecoregions with very low mean annual temperatures but no significant reductions in PPT observed since 1940 (*SI Appendix*, Figs. S8–S9). These conditions likely sustain adequate soil moisture, meaning an increase in air temperature may enhance tree growth rather than leading to drought stress (45). In contrast, we attribute the observed decrease in TRW at our most southerly sites in the S Plains to the significant increase in summer air temperatures, creating the potential for drought stress (46). From 1940 to 1980 s, black spruce radial growth showed less constraints for growth in the S Plains than at higher latitudes. However, since 1980 s, the species appears to have struggled to acclimate adequately to the excessive warmth recorded at these southern latitudes (Fig. 1*B*).

Overall, we found a lack of variation in TRW and the number of leaning events linked to the presence or absence of near-surface permafrost at the time of sampling in the Plains sites. This is probably attributable to changes in site permafrost status over the lifespan of the trees. Trends observed in northern environments over recent decades point to shorter-term periods of cooling and permafrost aggradation, superimposed on longer-term trends of warming and permafrost thaw/degradation (7, 8, 13). Indeed, changes in permafrost in our long-term permafrost monitoring sites since 2008 were predominantly unidirectional, characterized by a general increase in ALT (i.e., permafrost thaw) that aligns with these trends observed across northern environments in recent decades (19, 47, 48). Therefore, it is more likely that sites with permafrost within the rooting zone at the time of sampling had experienced these shallower permafrost conditions over the lifespan of the trees, and sites with no permafrost at the time of sampling, may have had shallower permafrost in the recent past that had degraded, but it will depend on when stands were established.

Significant differences in TRW and number of leaning events with the presence or absence of near-surface permafrost at the time of sampling in the Shield point to more stable permafrost conditions in that ecoregion, at least since 1980 s. This is because the Shield generally has coarser sediments, resulting in less ground ice compared to the fine-grained frost-susceptible material found overlying the sedimentary basin in the Plains (49). Lower tree growth in Shield near-surface permafrost sites was most likely linked to the challenges posed by the continued presence of permafrost over time, as cold and poorly drained soils limit tree growth (45), and the growth stress associated to seasonal thaw-driven tree leaning. The higher number of leaning events detected in Shield near-surface permafrost sites when compared with Shield sites with deep or no permafrost suggests that black spruce trees experienced higher number of leaning events in those stable permafrost sites.

Seasonal and long-term changes in ALT affect the foundation upon which trees grow. Continuous heaving and settlement cause the trees to frequently lean requiring corrective growth responses to maintain a vertical position. Tree response to leaning leaves a distinct signature in the rings of tree stems, characterized by the formation of reaction wood. Reaction wood (compression wood in black spruce trees) is characterized by higher lignin content that is triggered by the gravitational imbalance in leaning trees (34, 50). The production of such dense lignified wood requires greater allocation of carbon, i.e., higher sugar concentrations (51), which can adversely affect tree growth rates (52). By examining the radial patterns in NSC concentrations and their relationship with wood formation (TRW), we were able to assess the physiological mechanisms underlying the response of radial growth across different conditions of permafrost depths and stability. During the peak growing season, sugar concentrations in the stemwood were highest in the outermost rings and declined radially toward the inner rings for all trees (53–55), and the opposite pattern was found for starch concentrations (*SI Appendix*, Fig. S7). In boreal and temperate biomes, a strong depletion of starch is common during the growing season due to the high demand for carbohydrates to support growth and respiration (56–58). In contrast, soluble sugars serve important immediate physiological functions (e.g., osmotic regulation), with concentrations maintained above a critical threshold (59–61). This requirement to maintain relatively high sugar concentrations in forming rings appears to be particularly crucial for woody species in cold climates (57).

Every year, trees mobilize toward the inner rings the sugar reserves not used for growth or functional services. The significant correlations found between 1-y-old ring TRW and deeper sugar reserves suggest that trees can access reserves that are metabolically available on interannual timescales (62) (Fig. 3). Higher sugar reserves (lower rate of sugar depletion) were found in trees growing on near-surface or unstable permafrost sites (Fig. 4). This pattern is consistent with a conservative resource use strategy characterized by increased investment in sugar storage for future years and reduced new carbon sink. Lower radial growth and higher accumulation of carbon stored as NSCs in trees growing on near-surface permafrost may result from low rooting zone temperature impacting root function or nutrition during the growing season (10). However, we found that ground instability within the rooting zone in actively thawing permafrost environments appears to be even a more significant stressor affecting sugar reserves and consequently radial growth (Figs. 2 *C–E* and 4). These results highlight the importance of permafrost stability in modulating radial growth patterns, particularly in environments with widespread thaw processes. In contrast, the sharp depletion in sugars near the cambium in trees growing under less stressful environmental conditions (i.e., sites with deeper and stable permafrost tables) suggest a less conservative strategy, as trees are allocating proportionally more of their recently fixed carbon to growth in the outermost rings rather than to storage (63). Therefore, trees growing in sites with deep stable permafrost showed large, high-turnover carbohydrate pools, most likely fueling growth from a combination of assimilates from current and previous years (54, 64).

Future climate scenarios for the boreal region predict warmer and drier conditions (65), which may exacerbate the risk of carbon starvation and hydraulic failure (27), particularly at southern latitudes. A potential saturation in radial growth with continued warming may cause a reduction in photosynthetic C uptake (decreased photosynthesis), driving long-term growth declines, and enhancing mortality risk (45, 46, 66). This negative feedback

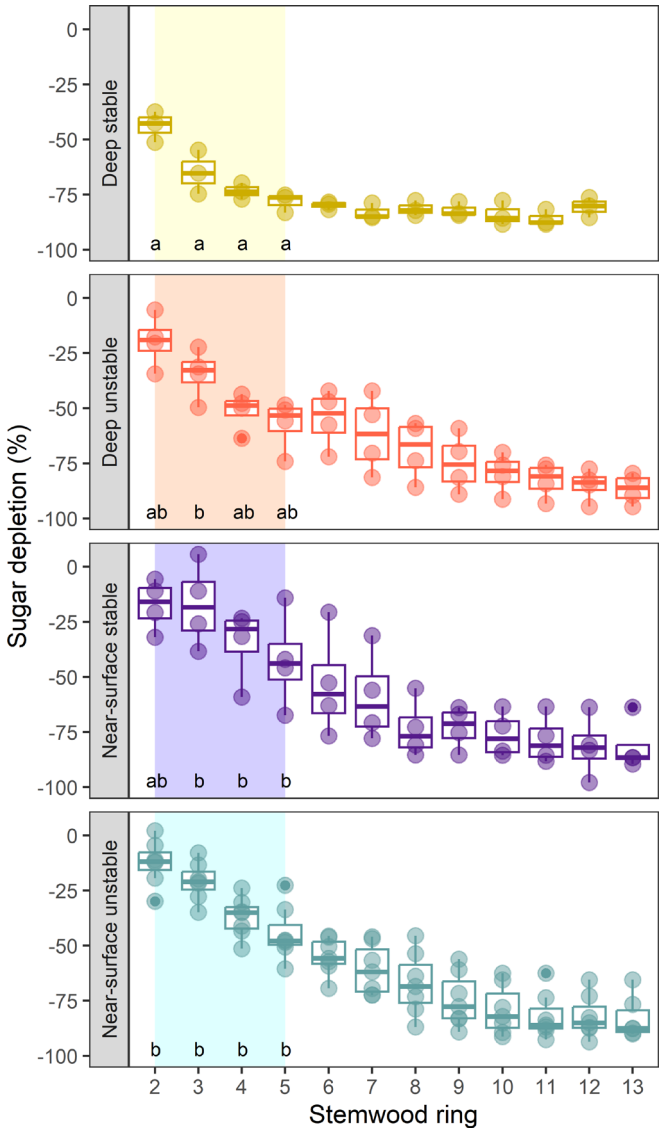

Fig. 4. Stemwood sugar depletion for contrasting permafrost conditions. Boxplots for 2 to 13-y-old stemwood sugar depletion relative to 1-y-old ring (%) for four levels of permafrost factor, i.e., sites with deep stable, near-surface stable, deep unstable, or near-surface unstable permafrost. Lowercase letters indicate significant differences among the four-level permafrost factor for each stemwood ring obtained in post hoc analyses. The colored areas indicate the stemwood rings with significant differences in the post hoc test (no significant differences were found among the four-level permafrost factor for stemwood rings 6 to 13). Circles are raw percentage of stemwood ring sugar depletion relative to 1-y-old ring (%) color-coded to indicate the four levels of permafrost factor.

would intensify in permafrost environments due to climate-driven changes in permafrost. Permafrost does not need to completely disappear for drought stress to occur; rather, the active layer only needs to become thick and well-drained enough to dry out, altering the rooting-zone soil conditions. However, this will depend on factors such as topography, material type, and drainage characteristics.

We suggest that any potential positive effect on tree growth from increased soil nutrients induced by warming-induced permafrost thaw seemed to be overshadowed by the stress in growth caused by ground instability in the plant rooting zone. Permafrost table instability drives trees to lean off-vertical repeatedly, significantly reducing radial growth in favor of more NSC reserves. However, longer monitoring is necessary to determine whether trees can recover from the physical disruption—or if they will succumb to it—once the ground is stabilized again, either because all the permafrost thaws, progresses below the rooting zone, or transitions into stable seasonal thaw.

Methods

Study Area and Field Sampling. Wood samples and permafrost data were collected in 109 sites dominated by black spruce [*P. mariana* (Mill.) B.S.P], in low subarctic and high-mid boreal forests in the Northwest Territories, Canada. Most of the sites were situated in the extensive discontinuous permafrost zone, while a few extend into the continuous and the sporadic permafrost zones (42) (Fig. 1).

Sites were stratified by level III ecoregions: the Northern and Southern Taiga Plains, henceforth N Plains and S Plains, and the Taiga Shield, henceforth Shield (67, 68). The Plains ecoregions are characterized by undulating glacial tills derived from Cretaceous sedimentary deposits, peatlands in wetter areas often underlain by permafrost, or glaciolacustrine sediments, particularly in the Mackenzie Valley (69). The Shield features hilly pre-Cambrian bedrock sparsely covered with thin layers of till, or lacustrine or aeolian deposits of clay, sand, or gravel (67, 68).

Ninety-four out of the 109 sites were established during summer fieldwork campaigns from 2016 to 2022 across the three ecoregions, in areas with no record of stand-replacing fire in recent history [>19 y postfire (70, 71)].

Fifteen out of 109 sites were established in the N Plains ecoregion in summer 2021, near to boreholes instrumented with thermistor strings, which allowed the study of historical changes in permafrost conditions, hereafter permafrost monitoring sites. The permafrost monitoring sites provided information on the texture of surficial materials (*SI Appendix*, Table S1*B* and see ref. 72 for more details). Most of the permafrost monitoring sites with shallow permafrost conditions were likely frost-susceptible, as they were underlain by peat or finer-grained sediments like silt or clay, which have high ice/moisture content and are prone to frost heave. In contrast, sites with deep permafrost were generally not frost-susceptible, as they were typically underlain by coarser sediments such as sand and gravel (even when there was a thin layer of peat at the surface). The permafrost monitoring sites also showed no record of recent stand-replacing fires. Stand-replacing crown fires are the most common fire regime in North America's boreal forests. However, a significant proportion of low-severity fires also occur within fire perimeters (73). We found evidence of fire-scarred trees at ten out of fifteen permafrost monitoring sites across various permafrost conditions (*SI Appendix*, Table S1*B* and Ref. 74; see section 3 for permafrost conditions), indicating the widespread occurrence of low-severity fires since the last stand-replacing fire.

In all sampled sites, we established one to three monitoring plots in representative landscape areas to collect wood samples and permafrost, soils, vegetation and forests stand attributes as part of a broader ecological research project in the NWT (70, 71). Each plot covered an area of 60 m^2 and consisted of two parallel 30-m transects running from south to north, positioned 2 m apart. Details about the sampling design can be found in refs. 70, 71. In the permafrost monitoring sites, the monitoring plots were established 30 to 50 m away from the boreholes to prevent disturbance in their measurements.

Wood Samples. In total, we collected wood samples from 961 live black spruce trees across the 109 sites, sampling 387 cores using increment borers, and 574 disks cutting the tree stems at the base of the tree (9 ± 4 trees sampled per site). Tree sampling focused on selecting black spruce trees that were most representative of the 60 m^2 monitoring plots at each site. However, wood samples were collected outside of these monitoring plots to avoid disturbance, as they were established as long-term permanent plots. As a result, our sampling design included a range of trees beyond just the dominant ones, which enhances the robustness of our inferences about the tree population.

Wood samples were used to determine tree age and to analyze climate-growth relationships, patterns in tree growth, reaction-wood dynamics (tree leaning events), and, in a subset of trees, stemwood NSC determination. Therefore, cores and disks were collected perpendicular to the stem axis, close to the base, where age estimation is most accurate and reaction wood reaches its maximum (34). The frequency of leaning events in trees growing in permafrost regions can inform about historical or current permafrost thaw dynamics. However, tree leaning events can only be assessed from disks, which represents the 57% of the tree-ring samples collected across the climatic gradient.

All cores and disks were processed following standard dendrochronological methods (75). Samples were scanned and annual Tree Ring Widths (TRW) were measured using CooRecorder (76). Cross-dating of individual series was checked using CooRecorder and COFECHA programs (77). In tree cores, usually two perpendicular radii of the trees were measured (1.8 ± 0.6 radius measured per tree). In the tree disks, at least two directions of the wood disk were measured, including the maximum and minimum wood radius, and often one or two more measurements in perpendicular directions to the major and minor axis (2.8 ± 0.6 radius measured per tree). Radii measurements were averaged to obtain the TRW for a given year for each tree and for studying tree leaning events in tree disks. Asymmetry in the width of concentric rings on a tree stem is an indicator of tree growth correcting for departures from a vertical orientation (lean). The annual intensity of tree leaning was defined as the ratio of maximum annual tree ring width to average annual tree ring width (modified from ref. 34), and was calculated by dividing the absolute maximum annual tree ring width from all the measured radius, by the average annual ring width of the rest of measurements. Tree leaning events were identified when the annual intensity of tree leaning was > 2. Then, the number of leaning events was counted per tree.

Stemwood NSC analyses were performed on an extra disk taken from each black spruce tree sampled at the 15 permafrost monitoring sites. The extra wood disks cut per tree were immediately frozen in the field on dry ice and then transported frozen to cold storage. Due to the time-consuming and costly nature of determining NSC concentrations, we analyzed a subset of disks, ensuring the selected trees covered a similar age range to minimize potential confounding effects and across contrasting permafrost conditions (see next section). The subset of frozen disks was first freeze-dried, and then annual rings from the period 2008–2020 were carefully separated by razor blade under a stereomicroscope. The samples were transferred to the University of Northern Arizona at Flagstaff, AZ, USA where concentrations of starch and sugars were determined, as percentages of dry weight. We followed protocols of ref. 78 for sugars and of ref. 79 for starch, as described in ref. 54. Sugar concentration was determined for 230 annual rings in 18 trees. Starch concentration was determined only for 36 annual rings in 15 trees instead that in the 230 annual rings, as our preliminary data showed very low concentrations of starch (0.038 ± 0.037 %; mean ± SD), and therefore there were not used for data analyses.

Permafrost Data.

Presence of near-surface permafrost and permafrost table depth. Information about the presence of near-surface permafrost and permafrost table depth was collected for 94 out of the 109 sites at the time of sampling using a 2 m length graduated steel rod with a handle, also known as frost probe. To do so, we pushed the steel rod into the soil down to the point of firm resistance, against the frost table or rocky ground. Probes typically cannot penetrate rocky ground and make a "ping" or scraping sound when encountering rock, rather than the "thump" when hitting permafrost. Sites that encountered frozen ground during the summer field campaigns were revisited at the end of the summer or early fall (late September and early October) to verify the presence of permafrost and to obtain the maximum thaw depth (80). We probed three to five times along the 30-meter east transect of each plot established per site to obtain a more accurate estimate of near-surface permafrost presence and an average measurement of thaw depth.

Sites were classified as near-surface permafrost sites if frozen ground was detected at the end of summer or early fall within the rooting zone (considered up to a depth of 2 m). The remaining sites were classified as sites with no permafrost in the upper two meters. We used the 2-meter permafrost table depth threshold for near-surface permafrost classification because it is unlikely that changes in permafrost table conditions below the plant rooting zone significantly impact black spruce forests, given the typical shallow depth of the rooting zone in this species (19).

Presence of near-surface permafrost, permafrost table depth, and permafrost table stability in permafrost monitoring sites. For the 15 permafrost monitoring sites, information about permafrost table depth was collected from the nearby boreholes instrumented with thermistor strings (Data available in ref. 81). The spacing between sensors is 0.5 m in the upper 2 m, increasing to usually 1 to 2 m at greater depths. ALT was estimated as the depth at which the maximum annual ground temperature was 0 °C (see refs. 19, 72, 82 for specific details about the data recording methods at the permafrost monitoring sites). The instrumentation provided continuous records of annual variation in (seasonally thawed) ALT from 2008 to 2018–2019 [the end of the time series varied per site; (81)]. Extreme increases or decreases in ALT within the time series at each site are due to small temperature fluctuations around 0 °C across the temperature profile, which are within the measurement error of the thermistors, and sometimes to larger spacing between thermistors (> 2 m), which affects the accuracy of the interpolation used to determine the thaw depth.

We classified permafrost monitoring sites as sites with near-surface permafrost, i.e., within the rooting zone, when maximum ALT values were shallower than 2 m depth for at least one year of the studied period. Permafrost monitoring sites with maximum active layers thicker than 2 m were classified as sites with deep permafrost.

To determine whether permafrost monitoring sites had stable or unstable permafrost tables, we used the annual ALT values in LMs as a function of year to test for trends over the studied period at all 15 sites. Only one site showed significant evidence of permafrost aggradation, or decrease of the ALT (slope coefficient -57.4 cm y^{-1}). In seven sites, the trend was positive (slope coefficients ranged from 7.40 to 56.6 cm y^{-1}), consistent with increase permafrost thaw or increasing of the ALT. Seven other sites showed no significant trends in ALT (*SI Appendix*, Fig. S3). Sites with significant absolute trends in ALT from 2008 to 2018–2019 were classified as sites with unstable permafrost and the remaining sites as sites with stable permafrost. We then defined a four-level permafrost factor to classify the depth and stability of the permafrost table in the 15 permafrost monitoring sites: sites with deep and stable permafrost table (n sites = 2), sites with near-surface and stable permafrost table (n sites = 5), sites with deep and unstable permafrost table (n sites = 3), and sites with near-surface and unstable permafrost table (n sites = 5).

Climate Data. We obtained historical time series of five climate variables (*SI Appendix*, Table S2) for the 109 sampling sites, using the ClimateNA v7.10 software (83). The historical data covered the period 1940–2020, the longest period for which consistent regional data were available (https://climate.weather.gc.ca). Seasonal means were calculated for the historical, normal, and future climatic variables following previous northern dendrochronology studies, e.g., ref. 36 where seasons were defined as winter (November–March), spring (April–May), Summer (June–August), and Autumn (September–October). We also obtained seasonal values of the same five variables for the 30-y normal period 1971–2000, and future values for 2011–2040, downscaled from the Coupled Model Intercomparison Project Phase 5 [CMIP5; (84)] under an intermediate emissions scenario, RCP4.5.

Temporal trends of the most influential seasonal climate variables for tree growth, obtained in climate-growth sensitivity analyses (see next section), were examined across regions by fitting linear and nonlinear regression models for each site between climate variables and year (Main results section). The temporal trend analyses covered the period from 1940 to 2020.

Climate Variable Selection for Tree Growth Analyses. For climate-growth analyses, we selected *798/961* trees from *104/109* sites having at least 31 continuous years of growth rings with paired annual climate and individual TRW data for the period 1940–2020. Climate variables included in these analyses were seasonal values from spring to winter at a lag of 1 y, and spring to autumn at lag 0, for the temperature variables average temperature, minimum temperature, maximum temperature, and moisture variables PPT and CMD (*SI Appendix*, Table S2).

We used generalized additive models (GAM) using functions gam and s of mgcv (85) R package to detrend the individual TRW series and all the site-level time-series seasonal climate variables. Detrending the tree growth series removes low-frequency variation related to nonclimatic drivers, such as growth, tree aging, and competition effects (86). Detrending the climate variables enhances the sensitivity of tree growth to interannual climate variations, a crucial consideration given observed trends in mean temperature over recent decades (87).

We used LM to test for associations between detrended, matched series of TRWs and climate variables. Separate models were fit using seasonal values from spring to winter from the current and previous year for a total of 44 seasonal covariates per tree (*SI Appendix*, Table S2). For each tree and covariate, we compared models with linear and quadratic adjustments selecting the best fit by Akaike information criterion (AIC), and then we selected the most sensitive temperature and PPT model by tree, i.e., the model with the lowest AIC. We then ranked the two groups of variables by selection frequency within ecoregions.

Statistical Analyses. In total, we built 11 statistical models including generalized additive mixed models (GAMM), Linear Mixed Effects Models (LMMs), general linear models (GLM), and LMs to analyze black spruce tree growth, leaning events, and NSCs (See next sections). GAMMs were fit using function gamm and s of mgcv (85) R package; LMMs, GLMs, and LMs were fit using function glmmTMB of glmmTMB R package (88). Specifications of the initial model formulas can be found below and summarized in *SI Appendix*, Table S3.

Tree growth analyses. We fit GAMM 1 to analyze the interannual variation in individual black spruce TRW as a response to climate, site permafrost status, while controlling for age and size effects. Models were fit separately for each ecoregion to account for systematic differences, such as surficial geology or parent material. We used natural logarithm of annual TRW as the response variable because of the skewed distributions of their values. Time series replication covered trees younger than 200 y old, from 1940 to 2020 for the Plains and from 1940 to 2017 for the Shield. This time series provided sufficient sample replication over time and within age classes, along with more reliable climate data. GAMM1 included as fixed effects the two-level permafrost factor (i.e., sites with near-surface permafrost *vs* no/deep permafrost), the primary climatic effects on tree growth obtained through climate-growth sensitivity analyses (See previous section, i.e., Summer Tmin and Summer CMD), annual cumulative basal diameter (reconstructed diameter based on tree rings) and cambial age (ring number from the pith) and calendar year to account for any temporal trends not explained by the climate variables (39, 86, 89). Primary climate drivers were included with quadratic terms to account for potential nonlinear responses of black spruce to climate (39, 66, 90). We introduced second interactions between first-order linear terms for climate drivers and permafrost factor, to explore whether tree growth patterns exhibited any associations with specific permafrost status of the sites at the time of sampling. Smoothing terms "s" were used for the cumulative diameter, cambial age, and calendar year variables. Smoothing terms represent cubic regression splines with a determined degree of smoothness (85). Random effects included tree identity and site to account for repeated measures and spatial variability. To account for temporal autocorrelation within trees, akin to traditional detrending methods, we used the continuous autocorrelation function corCAR1 (86) of mgcv (85) R package. Post hoc comparison of pairwise intercept differences between permafrost conditions within ecoregions was assessed using Wald tests, with the wald_gam function from the itsadug package (91).

We specified GAMM 2 to investigate the effects of absolute rates of permafrost change from 2008 to 2020 on TRW in the N Plains permafrost monitoring sites. GAMM 2 included as fixed effects the absolute rate of permafrost change, the annual cumulative diameter, and cambial age with smooth terms. Climatic variables and calendar year were not included in GAMM 2 to avoid collinearity effects between the rate of permafrost change with climatic variables and year.

GAMM 3 was specified to test for the effects of the four levels of permafrost factor from 2008 to 2020 on TRW in the N Plains permafrost monitoring sites. GAMM 3 included the same fixed and random effects than GAMM1 but included the four-level permafrost factor instead of the two-level factor.

We specified GAMM 8 to investigate the effects of the frequency of leaning events on TRW. Other fixed effects, such as climatic variables, were not included in GAMM 8 because our goal was to explore the generalized effect of the frequency of leaning events on tree growth using the longest available full time series, from 1723 to 2020. GAMM 8 included as fixed effects the number of leaning events per tree, the annual cumulative diameter, and cambial age with smooth terms.

GAMM 9 included the same fixed effects as GAMM 8, along with the number of leaning events per tree, annual cumulative diameter, cambial age with smooth terms, and climatic variables. As a result, the time series replication for this model spans from 1940 to 2020, aligning with the time series of climatic variables.

GAMMs 2, 3 and 8 and 9 used natural logarithm of annual TRW as the response variable and included the same random and autocorrelation effects as GAMM 1.

Lean events analyses. To analyze the relationship between the number of leaning events per tree and site rates of permafrost change, we run Spearman correlations between the total number of leaning events per tree and the absolute site-level rates of permafrost change from 2008 to 2018–2019 obtained in the 15 N Plains monitoring sites.

Our sample design, which included all trees within the monitoring plots–regardless of height or diameter, and beyond just the dominant trees–resulted in a very broad tree age distribution (*SI Appendix*, Fig. S1*B*). To determine whether the frequency of leaning varied with tree age, we run Spearman correlations between the total number of leaning events per tree and tree age, across the full climatic gradient. Results indicated a significant correlation (see the Results section). Consequently, we included age as a fixed predictor in the subsequent lean event analyses. We built GLM 4 to model the probability of the presence/absence of leaning events per tree using a binomial response (presence or absence of leaning events per tree) and GLM 5 to model the number of leaning events per tree using a negative binomial response as a function of tree age and the two-level permafrost factor. Models were fit separately for each ecoregion to account for systematic differences, such as surficial geology or parent material.

We specified GLM 6 to investigate the effects of absolute rates of permafrost change from 2008 to 2020 on the number of leaning events in the N Plains permafrost monitoring sites. GLM 6 included as fixed effects tree age and the absolute rate of permafrost change.

GLM 7 was specified to test for the effects of the four levels of permafrost factor from 2008 to 2020 on the number of leaning events in the N Plains permafrost monitoring sites. GLM 7 included as fixed effects tree age and the four-level permafrost factor.

Significant differences ($P < 0.05$) among levels of the two or four-level permafrost factor were examined using Tukey–Kramer Tukey post hoc tests with the lsmeans R package (92).

NSC analyses. NSCs were measured in the stemwood of black spruce trees growing over the four levels of permafrost factor in the N Plains permafrost monitoring sites. NSC concentrations were analyzed in stemwood samples divided into the first 13 individual rings, i.e., from 2008 to 2020 during the middle of the growing season (samples collected at the end of July 2021 when NSCs were still mobilized for growth). As all samples were collected during the same phenological stage for all trees, and no significant latitudinal or elevational gradients were considered for these analyses (Fig. 1), our data can be used to compare stemwood NSC concentrations among trees exposed by contrasting environmental conditions (93), i.e., the four levels of permafrost factor.

We analyzed the relationship between sugars and absolute ALT trends in LM 10, while controlling for age effects. The response variable for LM 10 was 1-y-old sugars. We analyzed 1-y-old sugars, instead of the mean sugar values from 2008 to 2018–2019 as we found a significant decrease in sugar concentrations (and a significant increase in starch) toward the pith (*Results*; *SI Appendix*, Fig. S7).

Next, we used Pearson correlations to explore the relationship between 1-y-old TRW and stemwood sugar content for each ring analyzed, i.e., 1 to 13 y old for sugars. We applied a Bonferroni correction, dividing our significant level $\alpha = 0.05$ by the number of tests (13 for sugars) to get the Bonferroni critical value of $P < 0.00385$. Significant correlations were then considered for these Bonferroni critical value. We avoid running separated Pearson correlation sets for the four levels of permafrost factor due to the limited number of NSC samples analyzed per year.

LMM 11 was specified to test for differences in the percentage of sugar depletion in stemwood rings from 2- to 13-y-old relative to new sugar content (1-y-old ring) among the four levels of permafrost factor. Time series replication covered the 2008–2020 period. We calculated the percentage of sugar depletion relative to new sugar content following this equation:

$$\text{Sugars relative to 1-y-old ring (\%)} = \left(\frac{(x \text{ years old sugars}) - (1 \text{ year old sugars})}{1 \text{ year old sugars}}\right) \times 100,$$

where x represents the stemwood rings from 2 to 13 y old.

LMM 11 included as fixed predictors the interactions between tree age and the four-level permafrost factor, and between the stemwood ring–as a factor–and the four levels of permafrost factor. Tree identity was included as random effect. Significant differences ($P < 0.05$) among levels of the four-level permafrost factor for each stemwood ring were examined using Tukey–Kramer Tukey post hoc tests with the lsmeans R package (92).

Model selection and model validation. Collinearity among fixed effects was explored in all the statistical models, using function vifstep of usdm (94) R package. We compared Akaike's information criterion (AIC) of candidate models using the logarithmic transformed and untransformed size and age variables against using smooth terms, after rerunning them using the maximum likelihood (ML) method. We selected the candidate models with lower AIC score. The final models were fitted using the restricted maximum likelihood method (95). Significance of the quadratic and interaction terms in the models was assessed comparing

the AIC between models containing and excluding each quadratic or interaction term using the ML method. Nonsignificant quadratic and interaction terms were manually removed from the models. Model validation for GAMMs was visually assessed by plotting the residuals against the fitted values. The model validation for LMMs, GLM, and LMs was conducted using the simulate Residuals function available in the DHARMa package (96). All statistics were carried out in R version 4.1.2 (97). All graphs were created using ggplot2 (98) or base R (97).

Data, Materials, and Software Availability. ALTs data from the permafrost monitoring sites are freely available on the Borealis online repository [(81); https://doi.org/10.5683/SP3/NCC40W]. Tree-ring data and NSC data are freely available on the Figshare online repository [(99); https://figshare.com/s/a86e06f14d1349eef9b7?file=46549639].

ACKNOWLEDGMENTS. We thank numerous students and technicians for field and lab assistance. We thank the GNWT Aurora Research Institute (Research License 15879). The Wilfrid Laurier University–GNWT Partnership Agreement was instrumental in providing logistical support and laboratory space. The permafrost monitoring in the Mackenzie River Valley is supported by Natural Resources Canada. RAS was supported by María Zambrano MZ2021 postdoctoral research program and the British Ecological Society (Small Research 2021–SR21/1291). Field sampling was supported by the Government of the Northwest Territories Environmental Studies Research Fund and Cumulative Impacts Monitoring Program (Project 170), Natural Science and Engineering Research Council Northern Supplement Funding, Polar Continental Shelf Program, and Northern Student Training Program. NSERC Discovery Grant support (J.F.J., J.L.B., and S.C.), Canada Research Chairs funding (J.L.B.), and in-kind support to J.F.J. from the Bonanza Creek LTER [funded by the US NSF (DEB-2224776) and the USDA Forest Service, Pacific Northwest Research Station] supported this work. The NSC analyses in this paper were conducted while R.A.-S. was a visiting scientist in the Center for Ecosystem Science and Society at Northern Arizona. We thank Emma Sherwood for her support with ArcMap and H. Brendan O'Neill from the Geological Survey of Canada, Natural Resources Canada, for providing comments on this manuscript.

Author affiliations: [a]Northern Forestry Centre, Canadian Forest Service, Natural Resources Canada, Edmonton, AB T6H 3S5, Canada; [b]Department of Biology, Wilfrid Laurier University, Waterloo, ON N2L 3C5, Canada; [c]Center for Ecosystem Science and Society, Northern Arizona University, Flagstaff, AZ 86011; [d]School of Informatics, Computing, and Cyber Systems, Northern Arizona University, Flagstaff, AZ 86011; [e]Geological Survey of Canada, Natural Resources Canada, Ottawa, ON K1A 0G1, Canada; [f]YukonU Research Centre, Yukon University, Whitehorse, YT Y1A 5K4, Canada; [g]Institute of Arctic Biology, University of Alaska Fairbanks, Fairbanks, AK 99775; [h]Renewable and Sustainable Energy Institute, Department of Ecology and Evolutionary Biology, University of Colorado Boulder, Boulder, CO 80309-0027; [i]Department of Wood and Forest Sciences, Laval University, Quebec City, QC G1V 0A6, Canada; and [j]LI-COR Biosciences, Lincoln, NE 68504

1. Y. Pan *et al.*, A Large and persistent carbon sink in the world's Forests. *Science* **333**, 988 (2011).
2. S. Gauthier, P. Bernier, T. Kuuluvainen, A. Z. Shvidenko, D. G. Schepaschenko, Boreal forest health and global change. *Science* **349**, 819–822 (2015).
3. M. Helbig, C. Pappas, O. Sonnentag, Permafrost thaw and wildfire: Equally important drivers of boreal tree cover changes in the Taiga Plains, Canada: Drivers of boreal tree cover changes. *Geophys. Res. Lett.* **43**, 1598–1606 (2016).
4. L. D. Hinzman *et al.*, Evidence and Implications of recent climate change in northern alaska and other arctic regions. *Clim. Change* **72**, 251–298 (2005).
5. M. Previdi, K. L. Smith, L. M. Polvani, Arctic amplification of climate change: a review of underlying mechanisms. *Environ. Res. Lett.* **16**, 093003 (2021).
6. S. L. Smith, H. B. O'Neill, K. Isaksen, J. Noetzli, V. E. Romanovsky, The changing thermal state of permafrost. *Nat. Rev. Earth Environ.* **3**, 10–23 (2022).
7. S. L. Smith *et al.*, "Permafrost" in *State of the Climate in 2023*, L. Druckenmiller, R. L. Thoman, T. A. Moon, Eds. (Special Online Supplement to the Bulletin of the American Meteorological Society, 2024), vol. **105**, No. 8, pp. S314–S317.
8. B. Fox-Kemper *et al.*, "Ocean, cryosphere and sea level change" in *Climate Change 2021: The Physical Science Basis. Contribution of Working Group I to the Sixth Assessment Report of the Intergovernmental Panel on Climate Change* (2021), pp. 1211–1362.
9. A. Cabon *et al.*, Cross-biome synthesis of source versus sink limits to tree growth. *Science* **376**, 758–761 (2022).
10. C. Körner, G. Hoch, A test of treeline theory on a montane permafrost island. *Arct. Antarct. Alp. Res.* **38**, 113–119 (2006).
11. P. Alvarez-Uria, C. Körner, Low temperature limits of root growth in deciduous and evergreen temperate tree species. *Funct. Ecol.* **21**, 211–218 (2007).
12. S. Rossi *et al.*, Critical temperatures for xylogenesis in conifers of cold climates. *Global Ecol. Biogeogr.* **17**, 696–707 (2008).
13. H. B. O'Neill, S. Smith, C. Burn, C. Duchesne, Y. Zhang, Widespread permafrost degradation and thaw subsidence in northwest canada. *J. Geophy. Res: Earth Surf.* **128**, e2023JF007262 (2023).
14. K. E. Nyland *et al.*, Long-term circumpolar active layer monitoring (calm) program observations in northern alaskan tundra. *Polar Geogr.* **44**, 167–185 (2021).
15. J. L. Baltzer, T. Veness, L. E. Chasmer, A. E. Sniderhan, W. L. Quinton, Forests on thawing permafrost: Fragmentation, edge effects, and net forest loss. *Global Change Biol.* **20**, 824–834 (2014).
16. L. C. R. Silva *et al.*, Tree growth acceleration and expansion of alpine forests: The synergistic effect of atmospheric and edaphic change. *Sci. Adv.* **2**, e1501302 (2016).
17. H. Kropp *et al.*, Shallow soils are warmer under trees and tall shrubs across Arctic and Boreal ecosystems. *Environ. Res. Lett.* **16**, 015001 (2021).
18. K. R. Miner *et al.*, Permafrost carbon emissions in a changing Arctic. *Nat. Rev. Earth Environ.* **3**, 55–67 (2022).
19. E. L. Ogden, S. G. Cumming, S. L. Smith, M. R. Turetsky, J. L. Baltzer, Permafrost thaw induces short-term increase in vegetation productivity in northwestern Canada. *Global Change Biol.* **29**, 5352–5366 (2023).
20. V. G. Salmon *et al.*, Nitrogen availability increases in a tundra ecosystem during five years of experimental permafrost thaw. *Glob Change Biol.* **22**, 1927–1941 (2016).
21. G. Blume-Werry, A. Milbau, L. M. Teuber, M. Johansson, E. Dorrepaal, Dwelling in the deep – strongly increased root growth and rooting depth enhance plant interactions with thawing permafrost soil. *New Phytol.* **223**, 1328–1339 (2019).
22. L. T. Berner, S. J. Goetz, Satellite observations document trends consistent with a boreal forest biome shift. *Global Change Biol.* **28**, 3275–3292 (2022).
23. D. Wei *et al.*, Plant uptake of CO_2 outpaces losses from permafrost and plant respiration on the Tibetan Plateau. *Proc. Natl. Acad. Sci. U.S.A.* **118**, e2015283118 (2021).
24. M. P. Girardin *et al.*, No growth stimulation of Canada's boreal forest under half-century of combined warming and CO_2 fertilization. *Proc. Natl. Acad. Sci. U.S.A.* **113**, E8406–E8414 (2016).
25. G. K. Phoenix, R. Treharne, Arctic greening and browning: Challenges and a cascade of complexities. *Global Change Biol.* **28**, 3481–3483 (2022).
26. Q. Liu *et al.*, Drought-induced increase in tree mortality and corresponding decrease in the carbon sink capacity of Canada's boreal forests from 1970 to 2020. *Global Change Biol.* **29**, 2274–2285 (2023).
27. N. McDowell *et al.*, Mechanisms of plant survival and mortality during drought: Why do some plants survive while others succumb to drought?. *New Phytol.* **178**, 719–739 (2008).
28. J. M. Cable *et al.*, Permafrost thaw affects boreal deciduous plant transpiration through increased soil water, deeper thaw, and warmer soils. *Ecohydrology* **7**, 982–997 (2014).
29. R. Patankar, W. L. Quinton, M. Hayashi, J. L. Baltzer, Sap flow responses to seasonal thaw and permafrost degradation in a subarctic boreal peatland. *Trees* **29**, 129–142 (2015).
30. A. E. Sniderhan, J. L. Baltzer, Growth dynamics of black spruce (*Picea mariana*) in a rapidly thawing discontinuous permafrost peatland: Growth Dynamics boreal peatlands. *J. Geophys. Res. Biogeosci.* **121**, 2988–3000 (2016).
31. S. C. Zoltai, W. W. Pettapiece, Tree distribution on perennially frozen earth hummocks. *Arct. Alp. Res.* **6**, 403 (1974).
32. S. C. Zoltai, Tree ring record of soil movements on permafrost. *Arct. Alp. Res.* **7**, 331 (1975).
33. S. V. Kokelj, C. R. Burn, C. Tarnocai, The Structure and dynamics of earth hummocks in the subarctic forest near inuvik, Northwest territories. *Canada. Arct. Antarct. Alp. Res.* **39**, 99–109 (2007).
34. K. Fujii, K. Yasue, Y. Matsuura, Tree ring evidence of rapid development of drunken forest induced by permafrost warming. *Global Change Biol.* **28**, 3920–3928 (2022).
35. S. Zoltai, S. Taylor, J. Jeglum, G. Mills, J. Johnson, "Wetlands of boreal Canada" in *Wetlands of Canada* (National Wetlands Working Group, Canada Committee on Ecological Classification, Polyscience Publications Inc., Montreal, QC, Canada, 1988), vol. chapter 4, pp. 97–154.
36. A. E. Sniderhan, S. D. Mamet, J. L. Baltzer, Non-uniform growth dynamics of a dominant boreal tree species (*Picea mariana*) in the face of rapid climate change. *Can. J. Forest Res.*, (2021), 10.1139/cjfr-2020-0188.
37. M. V. Bryukhanova *et al.*, The response of δ13C, δ18O and cell anatomy of Larix gmelinii tree rings to differing soil active layer depths. *Dendrochronologia* **34**, 51–59 (2015).
38. M. W. Miles, V. V. Miles, I. Esau, Varying climate response across the tundra, forest-tundra and boreal forest biomes in northern West Siberia. *Environ. Res. Lett.* **14**, 075008 (2019).
39. E. F. Nicklen, C. A. Roland, R. W. Ruess, T. Scharnweber, M. Wilmking, Divergent responses to permafrost and precipitation reveal mechanisms for the spatial variation of two sympatric spruce. *Ecosphere* **12**, e03622 (2021).
40. F. Chapin, E. Schulze, H. Mooney, The ecology and economics of storage in plants. *Annu. Rev. Ecol. Evol. Sys.* **21**, 423–447 (1990).
41. G. Hoch, The carbon supply of Picea abies trees at a Swiss montane permafrost site. *Plant Ecol. Diversity* **1**, 13–20 (2008).
42. J. A. Heginbottom, M. A. Dubreuil, P. A. Harker, "Canada-permafrost" in *National Atlas of Canada, 5th ed* (1995), MCR 4177, Plate 2.1.
43. J. K. Green, T. F. Keenan, The limits of forest carbon sequestration. *Science* **376**, 692–693 (2022).
44. F. Babst *et al.*, Twentieth century redistribution in climatic drivers of global tree growth. *Sci. Adv.* **5**, eaat4313 (2019).
45. A. Mirabel, M. P. Girardin, J. Metsaranta, D. Way, P. B. Reich, Increasing atmospheric dryness reduces boreal forest tree growth. *Nat. Commun.* **14**, 6901 (2023).
46. K. D. Dearborn, C. A. Wallace, R. Patankar, J. L. Baltzer, Permafrost thaw in boreal peatlands is rapidly altering forest community composition. *J Ecol.* **109**, 1452–1467 (2021).
47. O. A. Carpino, A. A. Berg, W. L. Quinton, J. R. Adams, Climate change and permafrost thaw-induced boreal forest loss in northwestern Canada. *Environ. Res. Lett.* **13**, 084018 (2018).
48. N. J. Pastick *et al.*, Spatiotemporal remote sensing of ecosystem change and causation across Alaska. *Global Change Biol.* **25**, 1171–1189 (2019).
49. H. B. O'Neill, S. Wolfe, C. Duchesne, R. Parker, Effect of surficial geology mapping scale on modelled ground ice in canadian shield terrain. *Cryosphere* **18**, 2979–2990 (2024).
50. S. Yamashita, M. Yoshida, H. Yamamoto, Relationship between development of compression wood and gene expression. *Plant Sci.* **176**, 729–735 (2009).

51. S. Ma *et al.*, Variations and determinants of carbon content in plants: a global synthesis. *Biogeosciences* **15**, 693–702 (2018).
52. J. Gril, D. Jullien, S. Bardet, H. Yamamoto, Tree growth stress and related problems. *J. Wood Sci.* **63**, 411–432 (2017).
53. G. Hoch, A. Richter, Ch. Körner, Non-structural carbon compounds in temperate forest trees. *Plant Cell Environ.* **26**, 1067–1081 (2003).
54. A. D. Richardson *et al.*, Distribution and mixing of old and new nonstructural carbon in two temperate trees. *New Phytol.* **206**, 590–597 (2015).
55. M. E. Furze *et al.*, Seasonal fluctuation of nonstructural carbohydrates reveals the metabolic availability of stemwood reserves in temperate trees with contrasting wood anatomy. *Tree Physiol.* **40**, 1355–1365 (2020).
56. T. T. Kozlowski, Carbohydrate Sources and Sinks in Woody Plants. *Bot. Rev.* **58**, 107–222 (1992).
57. J. Martínez-Vilalta *et al.*, Dynamics of non-structural carbohydrates in terrestrial plants: A global synthesis. *Ecol. Monogr.* **86**, 495–516 (2016).
58. H. A. Mooney, The carbon balance of plants. *Annu. Rev. Ecol. Sys.* **3**, 315–346 (1972).
59. M. C. Dietze *et al.*, Nonstructural carbon in woody plants. *Annu. Rev. Plant Biol.* **65**, 667–687 (2014).
60. N. G. McDowell *et al.*, The interdependence of mechanisms underlying climate-driven vegetation mortality. *Trends Ecol. Evol.* **26**, 523–532 (2011).
61. A. Sala, D. R. Woodruff, F. C. Meinzer, Carbon dynamics in trees: Feast or famine? *Tree Physiol.* **32**, 764–775 (2012).
62. A. Gessler, K. Treydte, The fate and age of carbon – Insights into the storage and remobilization dynamics in trees. *New Phytol.* **209**, 1338–1340 (2016).
63. M. Iturrate-Garcia *et al.*, Plant trait response of tundra shrubs to permafrost thaw and nutrient addition. *Biogeosciences* **17**, 4981–4998 (2020).
64. M. S. Carbone *et al.*, Age, allocation and availability of nonstructural carbon in mature red maple trees. *New Phytol.* **200**, 1145–1155 (2013).
65. IPCC, 2018: Global Warming of 1.5°C. An IPCC Special Report on the impacts of global warming of 1.5°C above pre-industrial levels and related global greenhouse gas emission pathways, in the context of strengthening the global response to the threat of climate change, sustainable development, and efforts to eradicate poverty, V. Masson-Delmotte *et al.*, Eds., in press.
66. E. F. Nicklen, C. A. Roland, R. W. Ruess, J. H. Schmidt, A. H. Lloyd, Local site conditions drive climate–growth responses of Picea mariana and Picea glauca in interior Alaska. *Ecosphere* **7**, e01507 (2016).
67. Ecosystem Classification Group, *Ecological Regions of the Northwest Territories – Taiga Shield* (Department of Environment and Natural Resources, Government of the Northwest Territories., 2008).
68. Ecosystem Classification Group, *Ecological Regions of the Northwest Territories – Taiga Plains* (Department of Environment and Natural Resources, Government of the Northwest Territories., 2009).
69. L. Dyke, G. R. Brooks, The physical environment of the Mackenzie Valley, Northwest Territories: A base line for the assessment of environmental change. Geological Survey of Canada. *Bulletin* **547**, 208 pp. (2000).
70. R. Alfaro-Sánchez *et al.*, What drives reproductive maturity and efficiency in serotinous boreal conifers?. *Front. Ecol. Evol.* **10**, 869130 (2022).
71. A. G. Jorgensen *et al.*, The influence of postfire recovery and environmental conditions on boreal vegetation. *Ecosphere* **14**, e4605 (2023).
72. S. L. Smith *et al.*, *Geotechnical Database and Descriptions of Permafrost Monitoring Sites Established 2006–07 in The Central and Southern Mackenzie Corridor* (Geological Survey of Canada, 2009).
73. N. H. F. French, J. Graham, E. Whitman, L. L. Bourgeau-Chavez, Quantifying surface severity of the 2014 and 2015 fires in the Great Slave Lake area of Canada. *Int. J. Wildland Fire* **29**, 892 (2020).
74. R. Alfaro-Sánchez, J. F. Johnstone, J. L. Baltzer, Low-severity fires in the boreal region: Reproductive implications for black spruce stands in between stand-replacing fire events. *Ann. Bot.*, mcae055 (2024).
75. J. H. Speer, *Fundamentals of Tree-Ring Research*. The University of Arizona Press, (2010).
76. Cybis Elektronik & Data AB, Cybis CooRecorder v9.8.0 and Cybis CDendro v9.8.0. (Saltsjobaden, Sweden, 2022). http://www.cybis.se/forfun/dendro/index.htm. Accessed 30 January 2022.
77. R. L. Holmes, Computer-assisted quality control in tree-ring dating and measurement. *Tree-ring bull.* **43**, 69–78 (1983).
78. P. S. Chow, S. M. Landhäusser, A method for routine measurements of total sugar and starch content in woody plant tissues. *Tree Physiol.* **24**, 1129–1136 (2004).
79. P. M. Wargo *et al.*, Measuring changes in stress and vitality indicators in limed sugar maple on the Allegheny Plateau in north-central Pennsylvania. *Can. J. Forest Res.* **32**, 629–641 (2002).
80. S. Smith *et al.*, "Permafrost: Permafrost and seasonally frozen ground" in *Terrestrial Essential Climate Variables for Climate Change Assessment, Mitigation and Adaptation*, R. Sessa, H. Dolman, Eds. (Food and Agricultural Organization of the United Nations, 2008).
81. E. Ogden, S. G. Cumming, S. L. Smith, M. Turetsky, J. L. Baltzer, Data for: Permafrost thaw induces short term increase in vegetation *productivity* in northwestern Canada. Borealis. https://doi.org/10.5683/SP3/NCC40W. Deposited 20 June 2023.
82. C. Duchesne, J. Chartrand, S. L. Smith, *Report on 2018 Field Activities and Collection of Ground-thermal and Active-layer Data in The Mackenzie Corridor, Northwest Territories* (Geological Survey of Canada, 2020).
83. T. Wang, A. Hamann, D. Spittlehouse, C. Carroll, Locally downscaled and spatially customizable climate data for historical and future periods for North America. *PLOS One* **11**, e0156720 (2016).
84. K. E. Taylor, R. J. Stouffer, G. A. Meehl, An overview of CMIP5 and the experiment design. *Bull. Am. Meteorol. Soc.* **93**, 485–498 (2012).
85. S. N. Wood, *Generalized Additive Models: An Introduction with R* (Chapman and Hall/CRC, ed. 2, 2017).
86. K. J. Anderson-Teixeira *et al.*, Joint effects of climate, tree size, and year on annual tree growth derived from tree-ring records of ten globally distributed forests. *Global Change Biol.* **28**, 245–266 (2022).
87. C. Ols *et al.*, Detrending climate data prior to climate–growth analyses in dendroecology: A common best practice?. *Dendrochronologia* **79**, 126094 (2023).
88. M. E. Brooks *et al.*, glmmTMB balances speed and flexibility among packages for zero-inflated generalized linear mixed modeling. *R. J.* **9**, 378–400 (2017).
89. M. Trouillier *et al.*, Size matters–A comparison of three methods to assess age- and size-dependent climate sensitivity of trees. *Trees* **33**, 183–192 (2019).
90. P. F. Sullivan, R. R. Pattison, A. H. Brownlee, S. M. P. Cahoon, T. N. Hollingsworth, Limited evidence of declining growth among moisture-limited black and white spruce in interior Alaska. *Sci. Rep.* **7**, 15344 (2017).
91. J. van Rij, M. Wieling, R. H. Baayen, H. van Rijn, itsadug: Interpreting time series and autocorrelated data using GAMMs (R package version 2.4, 2020).
92. R. V. Lenth, Least-squares means: The R package lsmeans. *J. Statist. Software* **69**, 1–33 (2016).
93. G. Hoch, C. Körner, Global patterns of mobile carbon stores in trees at the high-elevation tree line. *Global Ecol. Biogeogr.* **21**, 861–871 (2012).
94. B. Naimi, N. A. S. Hamm, T. A. Groen, A. K. Skidmore, A. G. Toxopeus, Where is positional uncertainty a problem for species distribution modelling. *Ecography* **37**, 191–203 (2014).
95. A. F. Zuur, Ed., *Mixed effects models and extensions in ecology with R* (Springer, 2009).
96. F. Hartig, DHARMa: Residual Diagnostics for Hierarchical (Multi-Level / Mixed) Regression Models (2020), https://github.com/florianhartig/dharma.
97. R Core Team, *R: A Language and Environment for Statistical Computing* (R Foundation for Statistical Computing, 2019).
98. H. Wickham, *ggplot2: Elegant Graphics for Data Analysis* (Springer-Verlag, New York, 2016).
99. R. Alfaro-Sánchez *et al.*, Data for: Permafrost instability negates the *positive* impact of warming temperatures on boreal radial growth. Figshare. https://figshare.com/s/a86e06f14d1349eef9b7. Deposited 12 November 2023.